

Research Article



# Melatonin Ameliorates L-NAME-Induced Preeclampsia and Associated Hepatic Injury in Rats via NRF2/GPX4/SRXN1-Mediated Ferroptosis Suppression

Khadijeh Vazifeshenas-Darmiyani<sup>1</sup> , Asghar Zarban<sup>2</sup>, Javad Mohiti-Ardakani<sup>1\*</sup> , Mehran Hosseini<sup>3\*</sup> 

<sup>1</sup>Department of Biochemistry and Molecular Biology, School of Medicine, Shahid Sadoughi University of Medical Sciences, Yazd, Iran

<sup>2</sup>Department of Clinical Biochemistry, School of Medicine, Birjand University of Medical Sciences, Birjand, Iran

<sup>3</sup>Department of Anatomical Sciences, School of Medicine, Kerman University of Medical Sciences, Kerman, Iran

## ARTICLE INFO

### Article History:

**Received:** August 6, 2025

**Revised:** September 10, 2025

**Accepted:** September 11, 2025

**ePublished:** January 5, 2026

### Keywords:

Ferroptosis, Liver diseases, Melatonin, Oxidative stress, Preeclampsia

## Abstract

**Background:** Ferroptosis, an iron-dependent cell death driven by lipid peroxidation, is implicated in the pathogenesis of various organ injuries. As preeclampsia threatens maternal liver health via this pathway, we investigated melatonin's anti-ferroptotic efficacy in an L-NAME-induced rat model of preeclampsia, focusing on its mechanistic modulation.

**Methods:** Preeclampsia was induced in timed-pregnant Wistar rats via daily subcutaneous injections of L-NAME (125 mg/kg) from gestational day (GD) 13 until delivery. Treatment groups received intraperitoneal melatonin (10 mg/kg/day) in either a short-term (STM; GD14 to delivery) or a long-term (LTM; GD14 to postpartum day 14) regimen. Evaluations were performed at 23 and 90 days postpartum (PPD23 and PPD90). Systolic blood pressure and 24-hour urinary protein excretion were quantified. Hepatic oxidative stress status was evaluated by measuring malondialdehyde (MDA) concentration alongside the activities of superoxide dismutase (SOD) and glutathione peroxidase (GPx). Hepatic gene expression of ferroptosis-related mediators was analyzed, including nuclear factor erythroid 2-related factor 2 (NRF2), solute carrier family 7 member 11 (SLC7A11), sulfiredoxin-1 (SRXN1), and glutathione peroxidase 4 (GPX4). A comprehensive histopathological examination of liver tissue was also performed.

**Results:** Melatonin treatment (STM and LTM) significantly attenuated L-NAME-induced hypertension and proteinuria at all time points ( $P < 0.001$ ). It suppressed hepatic oxidative stress, normalizing MDA levels (LTM at PPD90) and elevating SOD/GPx activities ( $p < 0.01$ ). Mechanistically, melatonin reversed the downregulation of ferroptosis-related genes (NRF2, SLC7A11, GPX4;  $P < 0.001$ ), with STM also upregulating SRXN1 at PPD23. LTM showed superior NRF2/GPX4 induction to STM at PPD90. Both melatonin regimens mitigated L-NAME-induced persistent hepatic damage, including ductular reactions and fibrosis.

**Conclusion:** This study demonstrates that melatonin exerts sustained protection against preeclampsia-induced hepatic injury by suppressing ferroptosis through the NRF2/GPX4/SRXN1 pathway. The treatment attenuated ductular reactions and restored redox balance.

## Introduction

Preeclampsia, a gestational hypertensive disorder of multifactorial etiology, represents a leading cause of maternal and fetal morbidity worldwide.<sup>1</sup> This complex syndrome, complicating 2-8% of pregnancies, is characterized by systemic vascular dysfunction with particular predilection for hepatic, renal, and neurological systems.<sup>2,3</sup> Current diagnostic criteria mandate new-onset hypertension (systolic blood pressure  $\geq 140$  mm Hg) concurrent with proteinuria emerging after 20 weeks' gestation in previously normotensive individuals.<sup>4</sup>

Although maternal symptoms of preeclampsia

typically subside after delivery or cesarean section (making pregnancy termination the definitive treatment as outlined in medical textbooks), emerging evidence indicates that preeclampsia may predispose mothers to long-term secondary complications years later.<sup>3</sup> The hepatic manifestations of preeclampsia warrant particular attention. While overt liver injury typically resolves postpartum, emerging data suggest persistent subclinical hepatocyte damage may serve as a harbinger of chronic liver pathology.<sup>5</sup> Longitudinal cohort studies demonstrate a significant association between preeclampsia and subsequent hepatic dysfunction, with risk persisting for

\*Corresponding Authors: Javad Mohiti-Ardakani, Email: mohiti@ssu.ac.ir; Mehran Hosseini, Emails: Mehranhosseini@yahoo.co.in; m.hosseini@kmu.ac.ir

© 2026 The Author(s). This is an open access article and applies the Creative Commons Attribution Non-Commercial License (<http://creativecommons.org/licenses/by-nc/4.0/>). Non-commercial uses of the work are permitted, provided the original work is properly cited.

decades postpartum.<sup>6,7</sup>

The molecular pathogenesis of preeclampsia remains incompletely elucidated. Recent investigations have identified ferroptosis, an iron-dependent, lipid peroxidation-mediated cell death pathway, as a potentially pivotal mechanism.<sup>8</sup> Central to this process is the downregulation of glutathione peroxidase 4 (GPX4), the principal enzyme responsible for neutralizing cytotoxic phospholipid hydroperoxides.<sup>9,10</sup> Given ferroptosis's established involvement in diverse hepatic pathologies,<sup>11</sup> therapeutic modulation of this pathway may offer novel opportunities for mitigating preeclampsia-associated liver injury.

Melatonin, an indoleamine with pleiotropic biological activities, has emerged as a promising therapeutic candidate in preeclampsia management. Clinical observations reveal significant melatonin deficiency in preeclamptic patients compared to normotensive gravidas,<sup>12</sup> while therapeutic administration demonstrates both safety and efficacy in ameliorating oxidative stress and endothelial dysfunction.<sup>13,14</sup> Preclinical models corroborate these findings, with melatonin administration attenuating key pathological features including hypertension, placental ischemia, and oxidative damage.<sup>15,16</sup>

Mounting evidence positions melatonin as a potential regulator of ferroptosis through multiple molecular pathways.<sup>17</sup> However, its capacity to prevent preeclampsia-induced long-term hepatic sequelae via ferroptosis modulation remains unexplored. This investigation employs an L-NAME-induced rat model of preeclampsia to systematically evaluate the long-term hepatoprotective effects of melatonin, with particular emphasis on the ferroptosis signaling axis (NRF2/GPX4/SLC7A11/SRXN1) as a putative mechanistic target.

## Methods

### Animals

All animal experiments in this study were conducted in compliance with the ARRIVE (Animal Research: Reporting of In Vivo Experiments) guidelines and received ethical approval from the Institutional Ethics Committee of Shahid Sadoughi University of Medical Sciences (approval code: IR.SSU.AEC.1403.021).

In the present study, 11-week-old Wistar rats (both sexes) were used. Prior to experimentation, the animals were acclimatized for one week under standard laboratory conditions ( $24 \pm 2$  °C, 35–45% humidity, 12-h light/dark cycle) without intervention to ensure environmental adaptation. Female rats were bred with age-compatible males at a 3:1 female-to-male ratio ( $n = 72$ ). The observation of sperm in vaginal smears 24 hours post-mating defined gestational day zero (GD0).

### Study design

Following pregnancy confirmation, 66 pregnant rats were randomly assigned to four experimental groups: control ( $n = 18$ ), preeclampsia model ( $n = 18$ ), short-

term melatonin therapy (STM,  $n = 15$ ), and long-term melatonin therapy (LTM,  $n = 15$ ). To induce preeclampsia, rats of the model, STM and LTM groups received daily subcutaneous injections of N( $\omega$ )-Nitro-L-arginine methyl ester hydrochloride (L-NAME; 125 mg/kg)<sup>18</sup> from GD13 to GD20.<sup>19</sup> Melatonin-treated rats (STM and LTM groups) additionally received daily intraperitoneal (i.p.) injection of melatonin (m5250 Sigma, 10 mg/kg)<sup>20</sup> for one week (STM group) or three weeks (LTM group), beginning on GD14.

To confirm the induction of preeclampsia on day 19 of pregnancy (GD19), six rats were randomly selected from each group and assessed for proteinuria and arterial blood pressure. For this assessment, six animals were randomly selected from both the control and model groups, while three rats each were analyzed from the STM and LTM groups (this differential sampling approach was implemented because both melatonin-treated groups received identical treatment protocols up to GD19).

To evaluate the short-term and long-term maternal hepatic complications of preeclampsia, primary sampling was conducted on postpartum day (PPD) 23 (after weaning/short-term) and PPD90 (long-term) in the studied groups.

### Measurement of 24-h urinary protein (24-hUP)

On GD19, PPD23, and PPD90, six rats per group were individually housed in metabolic cages for 24-hour urine collection. Total urine volume was measured, and protein concentration was quantified using the Asalab total urine protein assay kit according to the manufacturer's protocol.

### Measurement of arterial blood pressure

At each time point (GD19, PPD23, and PPD90), six rats per group were randomly selected for arterial blood pressure measurement as previously described.<sup>21</sup> Briefly, animals were anesthetized with an i.p. injection of ketamine/xylazine (80 mg/kg; 10 mg/kg),<sup>22</sup> followed by a midline cervical incision to expose the left common carotid artery. A heparinized saline-filled polyethylene catheter (0.5 mm diameter) was inserted into the carotid artery and advanced toward the aortic arch, then secured with a surgical suture. The catheter was connected to a PowerLab® data acquisition system (AD Instruments, Australia), and hemodynamic parameters were recorded continuously for 30 minutes per animal.

### Blood and tissue collection

Following hemodynamic measurements at PPD23 and PPD90, blood samples were collected via cardiac puncture for hepatic enzyme profiling. Liver tissues were processed for three analytical approaches: 1) histological preparation through fixation in 4% paraformaldehyde; 2) biochemical assessment via homogenization in phosphate-buffered saline (PBS) at a 1:10 (w/v) ratio for oxidative stress markers analysis; and 3) molecular studies using PBS-rinsed, liquid nitrogen-snap-frozen aliquots stored at -80

°C until RNA extraction and gene expression analysis.

### Measurement of serum liver enzymes

Blood samples were centrifuged at 2500 rpm for 10 minutes to obtain serum. Aspartate aminotransferase (AST) and alanine aminotransferase (ALT) were then quantified in serum samples using an automated biochemical analyzer (BS-800 Modular System, China) and commercial kits (Asalab, Iran).

### Assessment of lipid peroxidation and antioxidant enzymes

Lipid peroxidation in liver tissue homogenates was assessed by measuring malondialdehyde (MDA) levels. Hepatic MDA content was determined spectrophotometrically (532 nm) using the thiobarbituric acid (TBA) assay as previously described.<sup>23</sup> Briefly, homogenates were reacted with H<sub>3</sub>PO<sub>4</sub>/TBA (90 °C, 45 min), extracted with n-butanol, and measured against tetramethoxypropane standards.

Hepatic glutathione peroxidase (GPx) activity was quantified using a commercial assay kit (Navand Salamat Co., Iran) by spectrophotometrically tracking NADPH oxidation at 340 nm during the enzymatic conversion of reduced glutathione to oxidized glutathione.

Hepatic superoxide dismutase (SOD) activity was measured with a commercial assay kit (Navand Salamat Co., Iran) based on the enzyme's capacity to suppress pyrogallol autoxidation. In this assay, SOD competitively inhibits the oxygen-dependent conversion of pyrogallol into chromogenic products. The degree of reaction inhibition, quantified spectrophotometrically (420 nm), serves as a direct measure of SOD enzymatic activity in tissue homogenates.<sup>24</sup>

### Reverse transcription polymerase chain reaction (RT-PCR)

Total RNA was isolated from hepatic tissue samples employing the Parstus RNA extraction kit (Iran). RNA purity was verified spectrophotometrically (Biotek™, USA) by confirming an A260/A280 ratio ≥ 2.0. First-strand cDNA synthesis was performed using the Easy cDNA synthesis kit (Parstus, Iran). Quantitative RT-PCR analysis was conducted with gene-specific primers targeting sulfiredoxin1 (SRXN1), nuclear factor erythroid 2-related factor 2 (NRF2), glutathione peroxidase 4 (GPX4), and solute carrier family 7 member 11 (SLC7A11) transcripts, with GAPDH serving as the

endogenous reference gene (primer sequences provided in Table 1). Primers for SRXN1, NRF2, GPX4, SLC7A11, and GAPDH were adapted from previous studies.<sup>25-29</sup> They were checked using NCBI Primer-BLAST, ensuring specificity and optimal melting temperatures prior to RT-PCR analysis. All primer sets were rigorously validated for amplification specificity and efficiency. PCR amplification was performed in duplicate using a StepOnePlus™ Real-Time PCR System (Applied Biosystems, USA) with Ampliqon SYBR Green Master Mix (Denmark), under the following cycling conditions: 40 cycles of denaturation at 95 °C for 15 seconds followed by annealing/extension at 62-65 °C for 30 seconds. Relative gene expression was calculated by the 2<sup>-ΔΔCt</sup> method after normalization to GAPDH reference gene expression.<sup>27</sup>

### Histological assessments

Tissue samples were processed using standard histological protocols: paraffin embedding, sectioning at 5 μm thickness, and subsequent staining with hematoxylin and eosin (H&E) for morphological evaluation and Masson's trichrome (MT) for collagen deposition analysis. For each specimen, three randomly selected slides were examined under an Olympus BX41 light microscope (Japan), with high-resolution digital images captured using an Olympus DP12 camera (Japan). Histopathological evaluation was performed using a semi-quantitative scoring system assessing four key features: hemorrhage, inflammatory infiltration, congestion, and cellular degeneration. Each parameter was graded on a 5-point scale: 1 (normal), 2 (mild, ≤ 25% involvement), 3 (moderate, 26-50% involvement), 4 (severe, 51-75% involvement), and 5 (very severe, > 75% involvement).<sup>30</sup> The total histopathological score for each sample was calculated as the cumulative sum of all individual feature scores.<sup>31</sup> Collagen deposition was quantitatively assessed in MT-stained liver sections (400× magnification) using ImageJ software with color deconvolution algorithms. Results were calculated as the percentage of collagen-positive area per field and expressed as fold-change relative to control group values.

### Statistical analysis

Results are expressed as mean ± SD. All statistical analyses were performed in GraphPad Prism (v10.0) employing one-way ANOVA with appropriate post hoc testing (Tukey's test for equal variances or Dunnett's T3 test for unequal variances). A threshold of p < 0.05 was considered statistically significant.

**Table 1.** The primer pairs used for RT-qPCR analysis

| Gene           | Primer forward                | Primer reverse                 |
|----------------|-------------------------------|--------------------------------|
| GAPDH          | 5'-GTCATCCAGAGCTGAACGG-3'     | 5'-ACTTGGCAGGTTTCTCCAGG-3'     |
| NRF2           | 5'-GCTGCCATTAGTCAGTCGCTCTC-3' | 5'-ACCGTGCCTTCAGTGTGCTTC-3'    |
| SLC7A11        | 5'-CCATCATCATCGGCACCGTCATC-3' | 5'-TACTCCACAGGCAGACCAGAACAC-3' |
| GPX4           | 5'-TGTGTAATGGGGACGATGCC-3'    | 5'-ACGCAGCCGTTCTTATCAATG-3'    |
| Sulfiredoxin-1 | 5'-CCCAAGCGGTGACTACTAC-3'     | 5'-GGCAGGAATGGTCTCTCTGTG-3'    |

## Results

### Effects on blood pressure and urine protein

Figure 1 presents systolic blood pressure and urinary protein levels at GD19, PPD23, and PPD90. On GD19, preeclamptic rats exhibited significantly elevated systolic blood pressure and urinary protein excretion compared to controls ( $P < 0.001$ ). In contrast, the melatonin-treated group (5 days of melatonin administration) demonstrated significantly reduced blood pressure ( $P < 0.001$ ) and proteinuria ( $P = 0.005$ ) relative to the untreated preeclamptic model group.

On PPD23 and PPD90, systolic blood pressure and urinary protein levels remained significantly elevated in the preeclampsia model group compared to controls ( $P < 0.001$  for all). Both short- and long-term melatonin treatments significantly attenuated hypertension in preeclamptic rats compared to the model group ( $P < 0.001$ ). By PPD90, melatonin-treated rats (STM and LTM groups) achieved blood pressure levels comparable to controls ( $P > 0.05$ ).

Melatonin therapy also effectively normalized proteinuria at both PPD23 and PPD90 time points, with no significant differences observed between treated and control groups ( $P > 0.05$ ).

### Effects on MDA, SOD, and GPx

Lipid peroxidation was assessed by measuring MDA levels in hepatic tissues (Figure 2). The model group showed significantly elevated MDA concentrations compared to controls at both PPD23 ( $P = 0.002$ ) and PPD90 ( $P < 0.001$ ). Melatonin administration normalized hepatic MDA levels in preeclamptic rats by PPD23, regardless of treatment duration. However, by PPD90, only long-

term melatonin treatment (LTM group) completely restored hepatic MDA to control levels. While short-term melatonin therapy significantly reduced MDA compared to untreated model rats ( $P < 0.001$ ), these levels remained elevated relative to the control group ( $P < 0.001$ ).

SOD activity in hepatic tissue revealed significant differences between the studied groups (Figure 2). The model group demonstrated markedly reduced SOD levels compared to controls at both postpartum PPD23 and PPD90 ( $P < 0.001$  for both time points). At PPD23, melatonin administration produced a duration-dependent enhancement of SOD activity in preeclamptic rats. Treated animals not only surpassed model group levels ( $P < 0.001$ ) but also exceeded control values ( $P < 0.001$ ). The long-term melatonin regimen (LTM) yielded significantly higher SOD activity than short-term treatment ( $P < 0.001$ ). By PPD90, both melatonin regimens significantly restored SOD activity relative to untreated model rats ( $P < 0.001$ ). Short-term treatment normalized SOD to control levels ( $P > 0.05$  vs control), while long-term administration maintained supranormal activity ( $P = 0.009$  vs control).

Hepatic GPx activity was significantly reduced in the preeclampsia model group compared to controls at both PPD23 ( $P = 0.007$ ) and PPD90 ( $P < 0.001$ ) (Figure 2). At PPD23, melatonin treatment normalized GPx activity regardless of treatment duration, with no significant differences between STM and LTM groups or between treated animals and controls ( $P > 0.05$  for all comparisons). By PPD90, treatment duration significantly influenced outcomes. While both STM and LTM regimens enhanced GPx activity compared to untreated model rats ( $P < 0.001$ ), the LTM group demonstrated superior

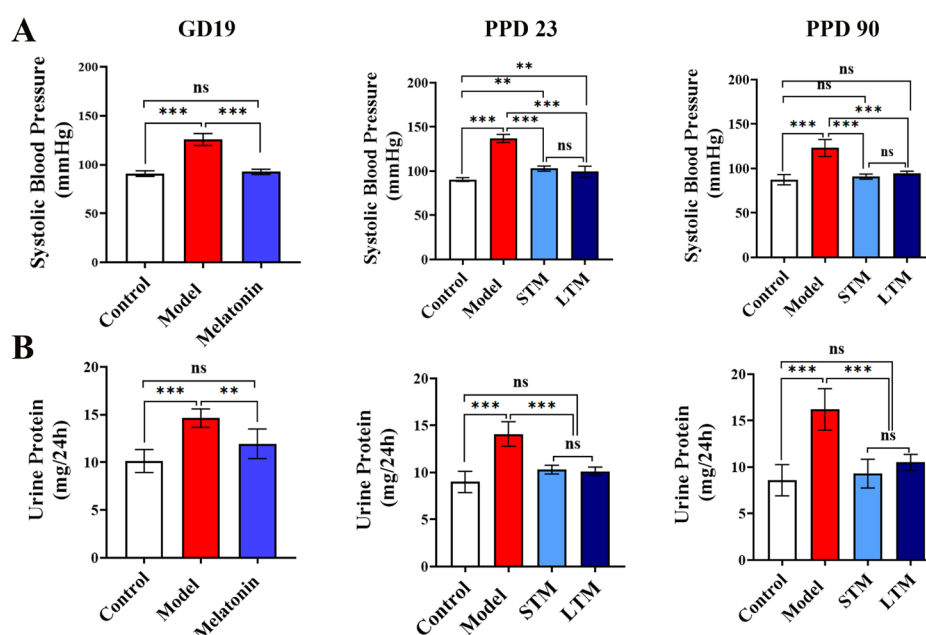


**Figure 1.** Effects of melatonin treatment on (A) systolic blood pressure and (B) 24-hour urinary protein excretion in preeclamptic rats at gestational day 19 (GD19), postpartum day 23 (PPD23), and PPD90. Groups: Model (L-NAME-induced preeclampsia, untreated); STM (short-term melatonin treatment, GD14 to delivery); LTM (long-term melatonin treatment, GD14 to PPD14). Data are presented as mean  $\pm$  SD. Differences were considered significant at  $**P < 0.01$  and  $***P < 0.001$  between groups

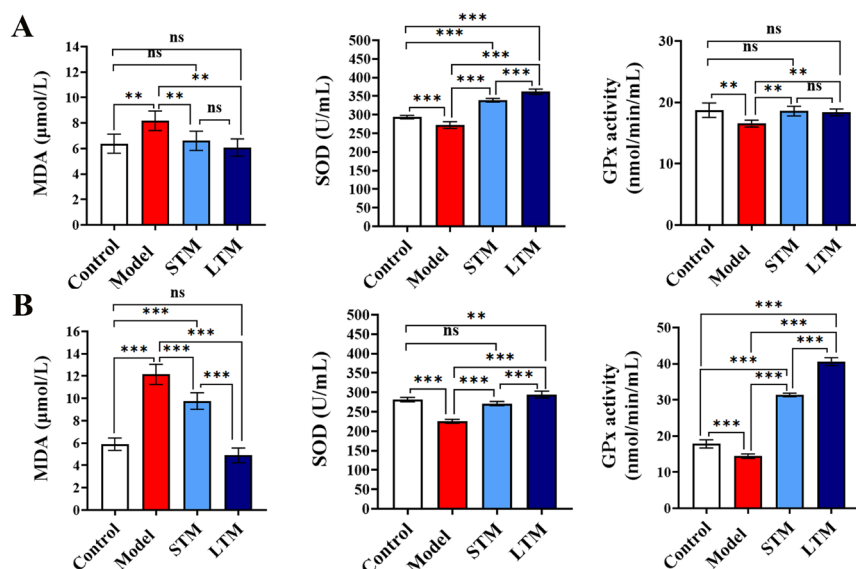


**Figure 2.** Effects of melatonin treatment on hepatic oxidative stress markers: (A) malondialdehyde (MDA) levels, superoxide dismutase (SOD) activity, and glutathione peroxidase (GPx) activity at postpartum day 23 (PPD23); (B) corresponding measurements at PPD90. Experimental groups: Model (L-NAME-induced preeclampsia, untreated); STM (short-term melatonin treatment, GD14 to delivery); LTM (long-term melatonin treatment, GD14 to PPD14). Data are presented as mean  $\pm$  SD. Differences were considered significant at  $**P < 0.01$  and  $***P < 0.001$  between groups

restoration ( $P < 0.001$  vs STM). Notably, both treatment groups ultimately exceeded control GPx activity levels ( $P < 0.001$ ).

#### Effects on ferroptosis-related gene expression

NRF2 gene expression analysis revealed significant effects of preeclampsia and melatonin treatment at both postpartum time points (Figure 3). Hepatic NRF2 expression was markedly suppressed in preeclamptic rats compared to controls at PPD23 and PPD90 ( $P < 0.001$  at both time points). At PPD23, melatonin treatment maintained NRF2 expression at control levels in preeclamptic rats ( $P > 0.05$  vs control), regardless of treatment duration. By PPD90, both STM and LTM groups exhibited significantly elevated NRF2 expression compared to both model and control groups ( $P < 0.01$  for all comparisons). Notably, STM treatment induced higher NRF2 expression than LTM at this stage ( $P < 0.001$ ).

At PPD23, hepatic SLC7A11 mRNA expression was significantly downregulated in preeclamptic rats relative to healthy controls ( $P < 0.001$ ). Both short- and long-term melatonin administration significantly attenuated this suppression compared to untreated model animals ( $P < 0.001$ ), though expression levels in treated groups remained below control values ( $P < 0.001$ ). By PPD90, no significant intergroup differences in SLC7A11 gene expression were observed ( $P > 0.05$ ).

Analysis of GPX4 gene expression revealed significant downregulation in preeclamptic rats compared to controls at both PPD23 and PPD90 ( $P < 0.001$ ; Figure 3). At PPD23, melatonin administration, irrespective of treatment duration, not only prevented GPX4 suppression ( $P < 0.001$  vs model group) but also induced supra-normal expression levels ( $P < 0.001$  vs controls). By PPD90, both treatment regimens maintained significantly elevated

GPX4 expression relative to untreated model animals ( $P < 0.001$ ). Notably, the LTM group demonstrated superior GPX4 induction compared to both STM treatment ( $P < 0.001$ ) and healthy controls ( $P < 0.001$ ).

SRXN1 gene expression analysis revealed distinct temporal patterns across study groups (Figure 3). At PPD23, hepatic SRXN1 expression was significantly suppressed in the model, STM, and LTM groups compared to the control group ( $P < 0.001$  for all comparisons). However, only the STM group exhibited significantly higher expression relative to the model group ( $P < 0.001$ ). By PPD90, while SRXN1 expression showed no significant difference between control and model groups, both melatonin treatment regimens induced significant overexpression compared to the control group (STM:  $P = 0.001$ ; LTM:  $P < 0.001$ ). Notably, the LTM group demonstrated superior SRXN1 induction versus both the STM and control groups ( $P < 0.001$ ).

#### Effects on liver enzymes and histopathology

The results of liver enzyme analyses are presented in Table 2. On PPD23, rats in the model group exhibited significantly elevated levels of AST and ALT compared to the control group ( $P < 0.001$ ). Only rats subjected to long-term melatonin treatment (LTM group) demonstrated a significant reduction in liver enzyme levels relative to the model group ( $P < 0.001$ ); however, their enzyme concentrations remained elevated compared to normal values ( $P < 0.001$  vs. control).

Histological evaluation of liver tissue on PPD23 revealed no discernible morphological differences among the studied groups (Figure 4A and 4B). Hematoxylin and eosin (H&E) staining analysis demonstrated no significant intergroup differences in hemorrhage, congestion, degeneration, or inflammation indices. In contrast, MT

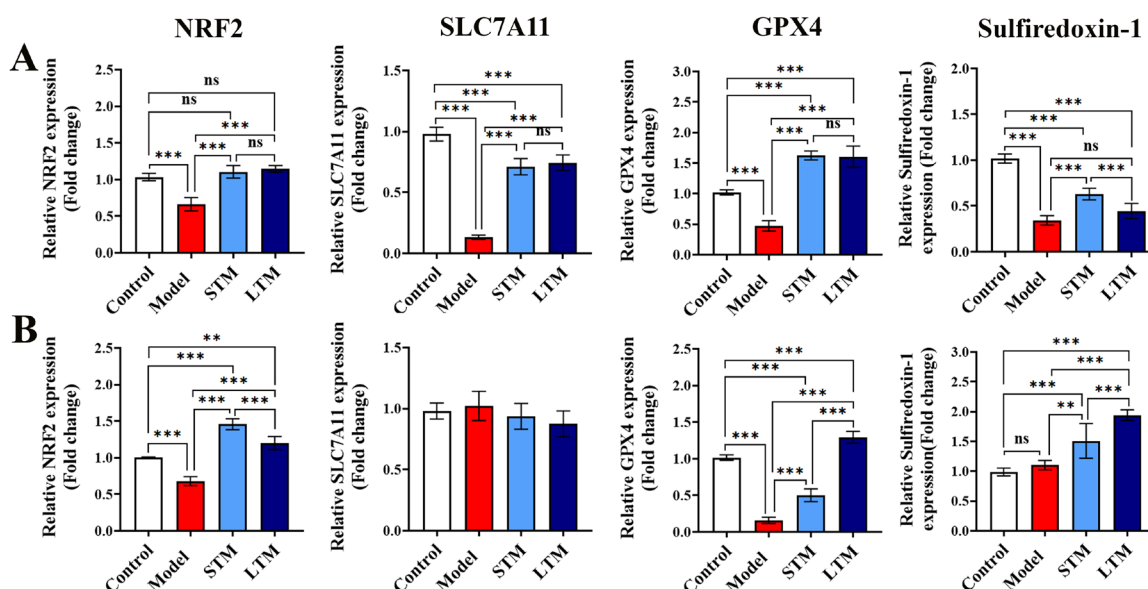


**Figure 3.** Hepatic mRNA expression of (A) NRF2, SLC7A11, GPX4, and sulfiredoxin-1 (SRXN1) at postpartum day 23 (PPD23) and (B) corresponding expression levels at PPD90. Experimental groups: Model (L-NAME-induced preeclampsia, untreated); STM (short-term melatonin treatment, GD14 to delivery); LTM (long-term melatonin treatment, GD14 to PPD14). Data are presented as mean  $\pm$  SD. Differences were considered significant at  $**P < 0.01$  and  $***P < 0.001$  between groups

**Table 2.** Effects of melatonin therapy during preeclampsia on postpartum liver enzymes

|        |           | Control           | Model                             | STM                                 | LTM                                      |
|--------|-----------|-------------------|-----------------------------------|-------------------------------------|--|
| PPD 23 | AST(IU/L) | 92.17 $\pm$ 15.39 | 185.5 $\pm$ 7.00 <sup>***</sup>   | 176.0 $\pm$ 10.14 <sup>***</sup>    | 138.2 $\pm$ 10.01 <sup>***,###,†††</sup> |
|        | ALT(IU/L) | 44.00 $\pm$ 9.25  | 172.28 $\pm$ 15.98 <sup>***</sup> | 155.3 $\pm$ 12.32 <sup>***</sup>    | 86.33 $\pm$ 11.33 <sup>***,###,†††</sup> |
| PPD 90 | AST(IU/L) | 90.33 $\pm$ 10.17 | 143.80 $\pm$ 9.16 <sup>***</sup>  | 119.8 $\pm$ 8.28 <sup>***,###</sup> | 111.2 $\pm$ 7.70 <sup>***</sup>          |
|        | ALT(IU/L) | 44.83 $\pm$ 9.10  | 119.70 $\pm$ 19.04 <sup>***</sup> | 51.50 $\pm$ 7.60 <sup>###</sup>     | 50.83 $\pm$ 13.59 <sup>###</sup>         |

Data are presented as mean  $\pm$  standard deviation (SD). Abbreviations: PPD, postpartum day; STM, short-term melatonin therapy; LTM, long-term melatonin therapy.  $***P < 0.001$  and  $**P < 0.01$  versus control group;  $###P < 0.001$  versus model group;  $†††P < 0.001$  versus STM group.

staining revealed distinct collagen deposition patterns between groups (Figures 4A and 4C). The model group exhibited significantly higher collagen fiber intensity in both portal spaces and central lobular veins compared to the control group ( $P < 0.001$ ; Figure 4C). Although melatonin treatment—irrespective of duration—significantly suppressed collagen bundle formation in hepatic tissue, staining intensity in these groups remained elevated relative to controls ( $P < 0.001$ ).

By PPD90, AST and ALT levels in the model group remained significantly higher than those in the control group ( $P < 0.001$ ). Notably, melatonin administration significantly attenuated liver enzyme elevations, irrespective of treatment duration ( $P < 0.001$ ). Furthermore, ALT levels in melatonin-treated rats did not differ significantly from those in the control group ( $P > 0.05$ ), indicating a restoration to baseline values.

Histological examinations on PPD90 using H&E staining revealed substantial morphological and pathological alterations among the experimental groups (Figure 5A). In the model group, the most prominent pathological feature was a pronounced ductal reaction, characterized by extensive proliferation of cholangiocyte-like cells, which imparted a distinct lobular architecture to the hepatic tissue. Additionally, multiple foci of

inflammatory cell infiltration were evident across most microscopic fields (Figure 5A). Consequently, the liver injury index in the model group was markedly elevated compared to all other groups ( $P < 0.001$ , Figure 5B). In contrast, melatonin-treated groups exhibited liver injury indices that were statistically indistinguishable from those of the control group.

The MT staining further demonstrated significantly greater collagen fiber deposition in the model group relative to controls ( $P < 0.001$ , Figure 5C). Notably, melatonin administration—irrespective of treatment regimen—effectively attenuated collagen fiber formation in hepatic tissue, resulting in staining intensities that were not significantly different from those observed in the control group.

## Discussion

The results of this study demonstrate that melatonin treatment significantly attenuated hypertension and proteinuria in preeclamptic rats at both 23 and 90 days postpartum. Melatonin treatment effectively mitigated the short- and long-term adverse effects of preeclampsia on oxidative stress markers, including MDA, SOD, and GPx. Furthermore, melatonin administration effectively modulated the ferroptosis pathway, thereby preventing

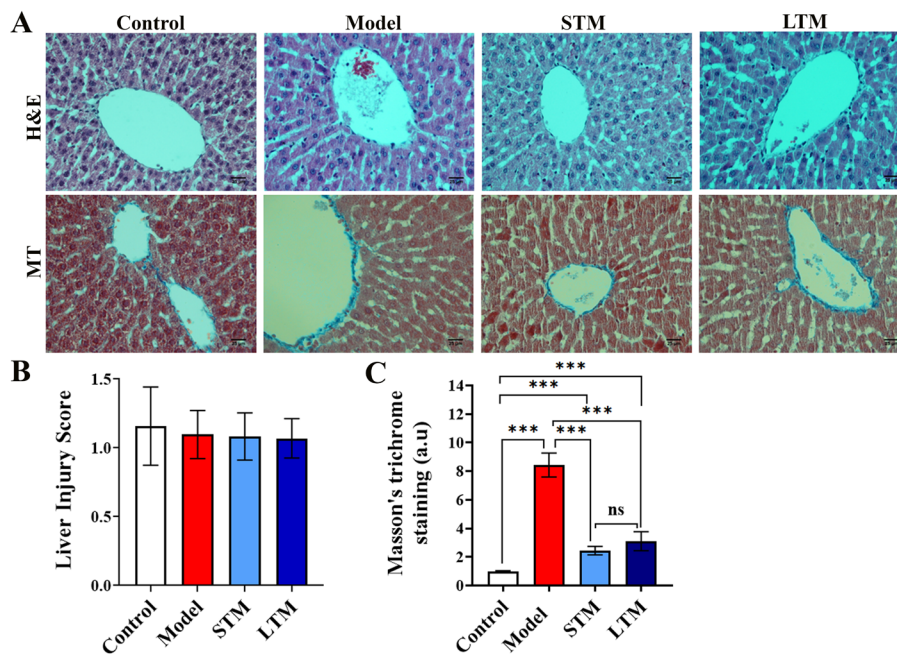


**Figure 4.** Histopathological analysis of liver tissue in preeclamptic rats at postpartum day 23. (A) Representative hematoxylin and eosin (H&E) and Masson's trichrome (MT)-stained sections (400× magnification; scale bar=25 μm). Experimental groups: Model (L-NAME-induced preeclampsia, untreated); STM (short-term melatonin treatment, GD14 to delivery); LTM (long-term melatonin treatment, GD14 to PPD14). (B) Semiquantitative liver injury scores based on H&E staining. (C) Quantitative analysis of collagen deposition (MT staining optical density). Data represent mean±SD. Differences were considered significant at \*\*\* $P < 0.001$  between groups

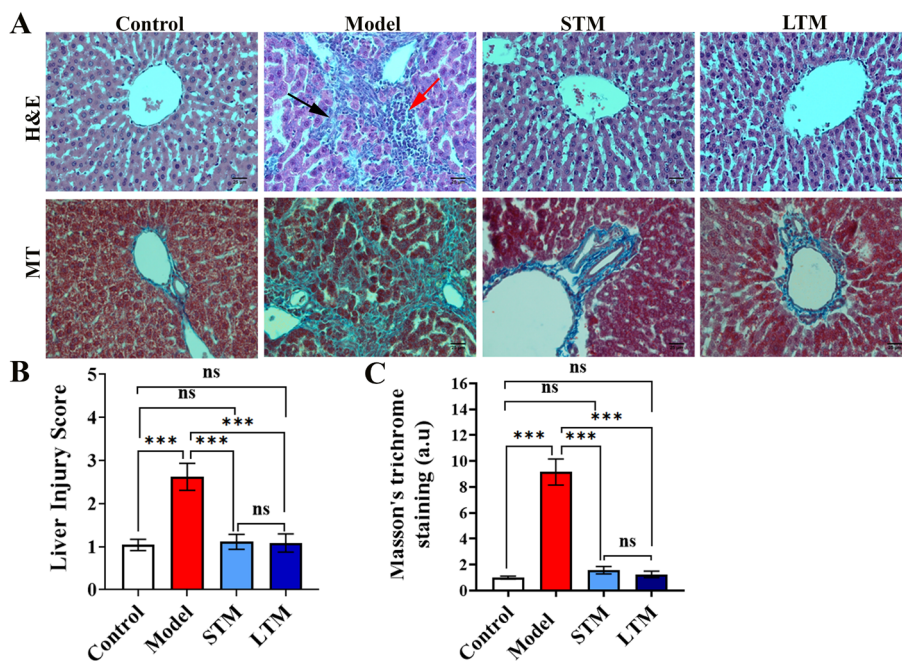


**Figure 5.** Histopathological evaluation of hepatic tissue in preeclamptic rats at postpartum day 90 (PPD90). (A) Representative photomicrographs of hematoxylin and eosin (H&E) and Masson's trichrome (MT)-stained liver sections (400× magnification; scale bar=25 μm). Black arrow indicates cholangiocyte-like cell proliferation (ductular reaction); red arrow denotes inflammatory cell infiltrates. Experimental groups: Model (L-NAME-induced preeclampsia, untreated); STM (short-term melatonin treatment, GD14 to delivery); LTM (long-term melatonin treatment, GD14 to PPD14). (B) Semiquantitative assessment of liver injury severity based on H&E-stained sections. (C) Quantitative evaluation of collagen deposition using MT-stained sections (optical density analysis). Data represent mean±SD. Differences were considered significant at \*\*\* $P < 0.001$  between groups

preeclampsia-induced long-term hepatic damage.

Our finding of sustained downregulation of the core ferroptosis regulators GPX4 and NRF2, alongside reduced SRXN1 expression, provides direct molecular evidence that ferroptosis is a key mechanism underlying the persistent hepatic injury observed in our preeclampsia

model. This aligns with the established paradigm that ferroptosis, driven by GPX4 inactivation and lethal lipid peroxidation, is implicated in the pathogenesis of preeclampsia.<sup>32-34</sup> Notably, melatonin administration (particularly long-term therapy) effectively reversed this molecular signature, preventing preeclampsia-induced

long-term hepatic damage, which supports the growing preclinical evidence that ferroptosis inhibitors can alleviate preeclampsia symptoms.<sup>34</sup>

The observed parallel downregulation of hepatic NRF2, GPX4, and SLC7A11 establishes a clear mechanistic link. This is highly significant given NRF2's pleiotropic role as a master transcriptional regulator of ferroptosis, governing cellular redox homeostasis by modulating glutathione metabolism (via SLC7A11 and GPX4), iron flux, and NADPH regeneration.<sup>35</sup> Furthermore, we investigated SRXN1 as a potential ferroptosis regulator in this context. The reduction in SRXN1 observed in our model may have exacerbated hepatic injury, as SRXN1 deficiency is known to promote fibrosis by dysregulating inflammasome activation.<sup>36</sup> The subsequent upregulation of SRXN1 by melatonin therapy is a notable finding, particularly as SRXN1 is a known transcriptional target of NRF2,<sup>37</sup> suggesting melatonin may act through NRF2 to restore a broad antioxidant defense network. The reduced NRF2 mRNA expression in the long-term melatonin group at PPD90 (vs. short-term) may reflect the successful resolution of oxidative stress, diminishing the need for sustained NRF2 upregulation.

Emerging research highlights melatonin's therapeutic potential for hepatic disorders through its multimodal action.<sup>38,39</sup> As a potent free radical scavenger, melatonin directly neutralizes reactive oxygen and nitrogen species while upregulating endogenous antioxidant systems via NRF2 activation, effectively countering oxidative liver damage.<sup>40</sup> Experimental models of non-alcoholic fatty liver disease demonstrate melatonin's unique capacity to inhibit ferroptotic cell death by maintaining glutathione homeostasis and preventing phospholipid peroxidation.<sup>17,41</sup>

The beneficial effects of melatonin on blood pressure, proteinuria, oxidative stress, and NRF2 expression observed in this study align with previous findings. Zuo and Jiang documented that prenatal melatonin treatment (10 mg/kg/day, i.p.) significantly reduced hypertension, proteinuria, and serum oxidative stress (MDA levels) in a preeclampsia rat model at GD19. The researchers also observed elevated placental NRF2 expression in melatonin-treated rats, leading them to propose that the hormone's mechanism involves the activation of key antioxidant defenses.<sup>16</sup> The experimental study conducted by Balarastaghi et al established that prolonged melatonin administration (10 mg/kg/day, i.p. injection for 28 consecutive days) significantly mitigated arsenic-induced pathological elevations in systolic blood pressure and attenuated oxidative stress biomarkers, as evidenced by reduced MDA levels and enhanced NRF2 expression.<sup>42</sup>

Our results demonstrated persistent systolic hypertension in model rats for up to three months postpartum following L-NAME withdrawal, suggesting enduring vascular dysfunction. These findings align with the work of Gaonkar et al, who reported sustained blood pressure elevation in rats 60 days after cessation

of low-dose L-NAME treatment (10-20 mg/kg/day for 3 weeks).<sup>43</sup> One key mechanism underlying persistent vascular dysfunction following L-NAME discontinuation appears to be the elevation of endothelium-derived constricting factor (EDCF). It has been previously reported that L-NAME administration disrupts nitric oxide (NO) signaling across arteries with large and small diameters. While NO bioavailability typically normalizes within three weeks post-treatment, structural remodeling and sustained EDCF overproduction in conduit arteries significantly delay systolic blood pressure recovery, even after NO synthesis restoration.<sup>44</sup>

Melatonin has established hepatoprotective properties with documented clinical safety during pregnancy and preeclampsia.<sup>12-14</sup> Our study advances this evidence by demonstrating melatonin's efficacy in attenuating both acute and chronic hepatic injury in a maternal rat preeclampsia model through dual modulation of antioxidant defenses and ferroptosis pathways. Specifically, we provide novel evidence that L-NAME-induced preeclampsia precipitates sustained liver damage persisting three months postpartum, histologically characterized by ductular reactions, a recognized precursor to fibrosis.<sup>45</sup> While this study focused on core ferroptosis markers (MDA, NRF2, GPX4, SLC7A11), further investigation of ancillary pathway components remains warranted. Although the L-NAME model is experimentally validated, its mechanistic divergence from human preeclampsia highlights the need for clinical translation, particularly regarding melatonin's therapeutic potential in post-preeclamptic women. Future studies should prioritize combinatorial regimens with standard therapies and comprehensive ferroptosis pathway analyses to optimize treatment strategies.

## Conclusion

In conclusion, this study demonstrates that melatonin effectively mitigates both short- and long-term hepatic complications in a rat model of preeclampsia by modulating oxidative stress and ferroptosis pathways. Our findings reveal that preeclampsia induces persistent liver injury, characterized by sustained lipid peroxidation, downregulation of GPX4, NRF2, and SRXN1, and histopathological evidence of ductular reactions. Melatonin administration, particularly long-term treatment, significantly attenuated these effects, reinforcing its role as a hepatoprotective agent. These results align with clinical evidence linking preeclampsia to chronic liver disease and highlight ferroptosis as a key mechanistic pathway. Future research should explore combinatorial therapies and additional ferroptosis markers to optimize treatment strategies for preeclampsia-related liver injury.

## Acknowledgements

We gratefully acknowledge Dr. Mehdi Shakibaei and Dr. Mansour Esmailidehaj for generously providing melatonin (standard) and L-NAME. We also extend our sincere appreciation to Mr. Hamid

Kabiri-Rad for his invaluable technical support in gene expression analysis.

#### Authors' Contribution

**Conceptualization:** Mehran Hosseini, Javad Mohiti-Ardakani.

**Formal analysis:** Mehran Hosseini

**Funding acquisition:** Javad Mohiti-Ardakani

**Investigation:** Khadijeh Vazifshenas-Darimiyan, Mehran Hosseini.

**Methodology:** Asghar Zarban, Mehran Hosseini.

**Project administration:** Javad Mohiti-Ardakani.

**Supervision:** Asghar Zarban, Mehran Hosseini.

**Validation:** Mehran Hosseini.

**Writing-original draft:** Khadijeh Vazifshenas-Darimiyan, Mehran Hosseini, Asghar Zarban, Javad Mohiti-Ardakani.

**Writing-Review & editing:** Mehran Hosseini.

#### Competing Interests

The authors declare that there is no conflict of interest

#### Data Availability Statement

The datasets used and/or analyzed during the present study are available from the corresponding author on reasonable request.

#### Ethical Approval

All procedures involving animals were carried out in consistent with the guideline of the Shahid Sadoughi University of Medical Sciences Ethics Committee (approval code: IR.SSU.AEC.1403.021). Guidelines as drawn up by the institutional review board were followed. The guidelines meet the requirements of the Declaration of Helsinki or comparable ethical standards.

#### Funding

This work was financially supported by Shahid Sadoughi University of Medical Sciences (Grant number: 18806). The funding body did not have any role in the design of the study, the collection, analysis and interpretation of the data or the writing of the manuscript.

#### References

- Chang KJ, Seow KM, Chen KH. Preeclampsia: recent advances in predicting, preventing, and managing the maternal and fetal life-threatening condition. *Int J Environ Res Public Health*. 2023;20(4):2994. doi: [10.3390/ijerph20042994](https://doi.org/10.3390/ijerph20042994).
- Macedo TC, Montagna E, Trevisan CM, Zaia V, de Oliveira R, Barbosa CP, et al. Prevalence of preeclampsia and eclampsia in adolescent pregnancy: A systematic review and meta-analysis of 291,247 adolescents worldwide since 1969. *Eur J Obstet Gynecol Reprod Biol*. 2020;248:177-86. doi: [10.1016/j.ejogrb.2020.03.043](https://doi.org/10.1016/j.ejogrb.2020.03.043).
- Dimitriadis E, Rolnik DL, Zhou W, Estrada-Gutierrez G, Koga K, Francisco RP, et al. Pre-eclampsia. *Nat Rev Dis Primers*. 2023;9(1):8. doi: [10.1038/s41572-023-00417-6](https://doi.org/10.1038/s41572-023-00417-6).
- Mei JY, Afshar Y. Hypertensive complications of pregnancy: hepatic consequences of preeclampsia through HELLP syndrome. *Clin Liver Dis (Hoboken)*. 2023;22(6):195-9. doi: [10.1097/cld.000000000000088](https://doi.org/10.1097/cld.000000000000088).
- Nelson DB, Byrne JJ, Cunningham FG. Acute fatty liver of pregnancy. *Clin Obstet Gynecol*. 2020;63(1):152-64. doi: [10.1097/grf.0000000000000494](https://doi.org/10.1097/grf.0000000000000494).
- Auger N, Jutras G, Paradis G, Ayoub A, Lewin A, Maniraho A, et al. Long-term risk of chronic liver disease after preeclampsia. *Int J Epidemiol*. 2025;54(3):dyaf072. doi: [10.1093/ije/dyaf072](https://doi.org/10.1093/ije/dyaf072).
- Nachshon S, Hadar E, Bardin R, Barbash-Hazan S, Borovich A, Braun M, et al. The association between chronic liver diseases and preeclampsia. *BMC Pregnancy Childbirth*. 2022;22(1):500. doi: [10.1186/s12884-022-04827-4](https://doi.org/10.1186/s12884-022-04827-4).
- Xu J, Zhou F, Wang X, Mo C. Role of ferroptosis in pregnancy related diseases and its therapeutic potential. *Front Cell Dev Biol*. 2023;11:1083838. doi: [10.3389/fcell.2023.1083838](https://doi.org/10.3389/fcell.2023.1083838).
- Beharier O, Tyurin VA, Goff JP, Guerrero-Santoro J, Kajiwaru K, Chu T, et al. PLA2G6 Guards placental trophoblasts against ferroptotic injury. *Proc Natl Acad Sci U S A*. 2020;117(44):27319-28. doi: [10.1073/pnas.2009201117](https://doi.org/10.1073/pnas.2009201117).
- Chen Z, Gan J, Zhang M, Du Y, Zhao H. Ferroptosis and its emerging role in pre-eclampsia. *Antioxidants (Basel)*. 2022;11(7):1282. doi: [10.3390/antiox11071282](https://doi.org/10.3390/antiox11071282).
- Chen J, Li X, Ge C, Min J, Wang F. The multifaceted role of ferroptosis in liver disease. *Cell Death Differ*. 2022;29(3):467-80. doi: [10.1038/s41418-022-00941-0](https://doi.org/10.1038/s41418-022-00941-0).
- Nakamura Y, Tamura H, Kashida S, Takayama H, Yamagata Y, Karube A, et al. Changes of serum melatonin level and its relationship to feto-placental unit during pregnancy. *J Pineal Res*. 2001;30(1):29-33. doi: [10.1034/j.1600-079x.2001.300104.x](https://doi.org/10.1034/j.1600-079x.2001.300104.x).
- Hobson SR, Gurusinghe S, Lim R, Alers NO, Miller SL, Kingdom JC, et al. Melatonin improves endothelial function in vitro and prolongs pregnancy in women with early-onset preeclampsia. *J Pineal Res*. 2018;65(3):e12508. doi: [10.1111/jpi.12508](https://doi.org/10.1111/jpi.12508).
- Langston-Cox A, Marshall SA, Lu D, Palmer KR, Wallace EM. Melatonin for the management of preeclampsia: a review. *Antioxidants (Basel)*. 2021;10(3):376. doi: [10.3390/antiox10030376](https://doi.org/10.3390/antiox10030376).
- Sun Y, Wang C, Zhang N, Liu F. Melatonin ameliorates hypertension in hypertensive pregnant mice and suppresses the hypertension-induced decrease in Ca(2+)-activated K<sup>+</sup> channels in uterine arteries. *Hypertens Res*. 2021;44(9):1079-86. doi: [10.1038/s41440-021-00675-5](https://doi.org/10.1038/s41440-021-00675-5).
- Zuo J, Jiang Z. Melatonin attenuates hypertension and oxidative stress in a rat model of L-NAME-induced gestational hypertension. *Vasc Med*. 2020;25(4):295-301. doi: [10.1177/1358863x20919798](https://doi.org/10.1177/1358863x20919798).
- Zhang D, Jia X, Lin D, Ma J. Melatonin and ferroptosis: mechanisms and therapeutic implications. *Biochem Pharmacol*. 2023;218:115909. doi: [10.1016/j.bcp.2023.115909](https://doi.org/10.1016/j.bcp.2023.115909).
- Shu W, Li H, Gong H, Zhang M, Niu X, Ma Y, et al. Evaluation of blood vessel injury, oxidative stress and circulating inflammatory factors in an L-NAME-induced preeclampsia-like rat model. *Exp Ther Med*. 2018;16(2):585-94. doi: [10.3892/etm.2018.6217](https://doi.org/10.3892/etm.2018.6217).
- Chen YH, Chang YC, Wu WJ, Chen M, Yen CC, Lan YW, et al. Kefir peptides mitigate L-NAME-induced preeclampsia in rats through modulating hypertension and endothelial dysfunction. *Biomed Pharmacother*. 2024;180:117592. doi: [10.1016/j.biopha.2024.117592](https://doi.org/10.1016/j.biopha.2024.117592).
- El-Malkey NF, Aref M, Emam H, Khalil SS. Impact of melatonin on full-term fetal brain development and transforming growth factor- $\beta$  level in a rat model of preeclampsia. *Reprod Sci*. 2021;28(8):2278-91. doi: [10.1007/s43032-021-00497-3](https://doi.org/10.1007/s43032-021-00497-3).
- Hassanzadeh-Taheri M, Mohammadifard M, Erfanian Z, Hosseini M. The maternal reduced uteroplacental perfusion model of preeclampsia induces sexually dimorphic metabolic responses in rat offspring. *Biol Sex Differ*. 2022;13(1):48. doi: [10.1186/s13293-022-00458-8](https://doi.org/10.1186/s13293-022-00458-8).
- Mesbahzadeh B, Moodi N, Hassanzadeh-Taheri M, Saheli M, Hosseini M. Therapeutic potential of tadalafil in acetic acid-induced gastric ulcer in rats: mechanisms and outcomes. *Naunyn Schmiedebergs Arch Pharmacol*. 2025. doi: [10.1007/s00210-025-04371-w](https://doi.org/10.1007/s00210-025-04371-w).
- Foadoddini M, Javdani H, Farahi A, Hosseini M. Therapeutic potential of *Ferula foetida* (Bunge) Regel on gastric ulcer model in rats. *Environ Sci Pollut Res Int*. 2022;29(8):12147-56. doi: [10.1007/s11356-021-16687-0](https://doi.org/10.1007/s11356-021-16687-0).
- Ahmadi-Zohan A, Hassanzadeh-Taheri M, Hosseini M. The effects of rosmarinic acid on hippocampal oxidative stress

- markers in LPS-induced neuroinflammation rats: rosmarinic acid and hippocampal oxidative stress. *Iran J Pharm Sci.* 2021;17(2):117-28. doi: [10.22037/ijps.v17.40290](https://doi.org/10.22037/ijps.v17.40290).
25. Du R, Cheng X, Ji J, Lu Y, Xie Y, Wang W, et al. Mechanism of ferroptosis in a rat model of premature ovarian insufficiency induced by cisplatin. *Sci Rep.* 2023;13(1):4463. doi: [10.1038/s41598-023-31712-7](https://doi.org/10.1038/s41598-023-31712-7).
26. Fathi R, Akbari A, Nasiri K, Chardahcherik M. Ginger (*Zingiber officinale* Roscoe) extract could upregulate the renal expression of NRF2 and TNF $\alpha$  and prevents ethanol-induced toxicity in rat kidney. *Avicenna J Phytomed.* 2021;11(2):134-45.
27. Hassanzadeh-Taheri M, Hayati S, Mohammadifard M, Hosseini M. Resveratrol prevents lipopolysaccharide-induced cognitive impairment in rats through regulation of hippocampal GluA1-containing AMPA receptors. *Pharm Sci.* 2021;28(3):383-93. doi: [10.34172/ps.2021.61](https://doi.org/10.34172/ps.2021.61).
28. Krümmel B, Plötz T, Jörns A, Lenzen S, Mehmeti I. The central role of glutathione peroxidase 4 in the regulation of ferroptosis and its implications for pro-inflammatory cytokine-mediated beta-cell death. *Biochim Biophys Acta Mol Basis Dis.* 2021;1867(6):166114. doi: [10.1016/j.bbadis.2021.166114](https://doi.org/10.1016/j.bbadis.2021.166114).
29. Yu S, Wang X, Lei S, Chen X, Liu Y, Zhou Y, et al. Sulfiredoxin-1 protects primary cultured astrocytes from ischemia-induced damage. *Neurochem Int.* 2015;82:19-27. doi: [10.1016/j.neuint.2015.01.005](https://doi.org/10.1016/j.neuint.2015.01.005).
30. Hassanzadeh-Taheri M, Hosseini M, Salimi M, Moodi H, Dorranpour D. Acute and sub-acute oral toxicity evaluation of *Astragalus hamosus* seedpod ethanolic extract in Wistar rats. *Pharm Sci.* 2018;24(1):23-30. doi: [10.15171/ps.2018.05](https://doi.org/10.15171/ps.2018.05).
31. Abedini MR, Paki S, Mohammadifard M, Foadoddini M, Vazifeshenas-Darmiyan K, Hosseini M. Evaluation of the in vivo and in vitro safety profile of *Cuscuta epithimum* ethanolic extract. *Avicenna J Phytomed.* 2021;11(6):645-56. doi: [10.22038/ajp.2021.18529](https://doi.org/10.22038/ajp.2021.18529).
32. Shan Y, Guan C, Wang J, Qi W, Chen A, Liu S. Impact of ferroptosis on preeclampsia: a review. *Biomed Pharmacother.* 2023;167:115466. doi: [10.1016/j.biopha.2023.115466](https://doi.org/10.1016/j.biopha.2023.115466).
33. Peng X, Lin Y, Li J, Liu M, Wang J, Li X, et al. Evaluation of glutathione peroxidase 4 role in preeclampsia. *Sci Rep.* 2016;6:33300. doi: [10.1038/srep33300](https://doi.org/10.1038/srep33300).
34. Shao Y, Zhang N, Xu T, Zhao M, Liu K. Ferroptosis in obstetrical and gynecological diseases: a mini review. *Front Biosci (Landmark Ed).* 2024;29(8):282. doi: [10.31083/j.fbl2908282](https://doi.org/10.31083/j.fbl2908282).
35. Yan R, Lin B, Jin W, Tang L, Hu S, Cai R. NRF2, a superstar of ferroptosis. *Antioxidants (Basel).* 2023;12(9):1739. doi: [10.3390/antiox12091739](https://doi.org/10.3390/antiox12091739).
36. Kim JW, Tung HC, Ke M, Xu P, Cai X, Xi Y, et al. The desulfinylation enzyme sulfiredoxin-1 attenuates HSC activation and liver fibrosis by modulating the PTPN12-NLRP3 axis. *Hepatology.* 2025;82(1):92-109. doi: [10.1097/hep.0000000000001133](https://doi.org/10.1097/hep.0000000000001133).
37. Wu KC, Liu JJ, Klaassen CD. Nrf2 activation prevents cadmium-induced acute liver injury. *Toxicol Appl Pharmacol.* 2012;263(1):14-20. doi: [10.1016/j.taap.2012.05.017](https://doi.org/10.1016/j.taap.2012.05.017).
38. Che Z, Song Y, Xu C, Li W, Dong Z, Wang C, et al. Melatonin alleviates alcoholic liver disease via EGFR-BRG1-TERT axis regulation. *Acta Pharm Sin B.* 2023;13(1):100-12. doi: [10.1016/j.apsb.2022.06.015](https://doi.org/10.1016/j.apsb.2022.06.015).
39. Dorranipour D, Pourjafari F, Malekpour-Afshar R, Basiri M, Hosseini M. Assessment of melatonin's therapeutic effectiveness against hepatic steatosis induced by a high-carbohydrate high-fat diet in rats. *Naunyn Schmiedebergs Arch Pharmacol.* 2024;397(5):2971-85. doi: [10.1007/s00210-023-02784-z](https://doi.org/10.1007/s00210-023-02784-z).
40. Zhu L, Zhang Q, Hua C, Ci X. Melatonin alleviates particulate matter-induced liver fibrosis by inhibiting ROS-mediated mitophagy and inflammation via Nrf2 activation. *Ecotoxicol Environ Saf.* 2023;268:115717. doi: [10.1016/j.ecoenv.2023.115717](https://doi.org/10.1016/j.ecoenv.2023.115717).
41. Saha M, Das S, Manna K, Saha KD. Melatonin targets ferroptosis through bimodal alteration of redox environment and cellular pathways in NAFLD model. *Biosci Rep.* 2023;43(10):BSR20230128. doi: [10.1042/bsr20230128](https://doi.org/10.1042/bsr20230128).
42. Balarastaghi S, Barangi S, Hosseinzadeh H, Imenshahidi M, Moosavi Z, Razavi BM, et al. Melatonin improves arsenic-induced hypertension through the inactivation of the Sirt1/autophagy pathway in rat. *Biomed Pharmacother.* 2022;151:113135. doi: [10.1016/j.biopha.2022.113135](https://doi.org/10.1016/j.biopha.2022.113135).
43. Gaonkar R, Pritmani J, Datar M, Singh D, Balasinar N, Nishi K. Long-term effects of sub-chronic exposure to L-NAME on reproductive system of male rats. *Naunyn Schmiedebergs Arch Pharmacol.* 2025;398(5):5303-19. doi: [10.1007/s00210-024-03609-3](https://doi.org/10.1007/s00210-024-03609-3).
44. Paulis L, Zicha J, Kunes J, Hojna S, Behuliak M, Celec P, et al. Regression of L-NAME-induced hypertension: the role of nitric oxide and endothelium-derived constricting factor. *Hypertens Res.* 2008;31(4):793-803. doi: [10.1291/hypres.31.793](https://doi.org/10.1291/hypres.31.793).
45. Sato K, Marzioni M, Meng F, Francis H, Glaser S, Alpini G. Ductular reaction in liver diseases: pathological mechanisms and translational significances. *Hepatology.* 2019;69(1):420-30. doi: [10.1002/hep.30150](https://doi.org/10.1002/hep.30150).